Leukemia (2007) 21, 2519–2526

www.nature.com/leu

ORIGINAL ARTICLE

Biological pathways and *in vivo* antitumor activity induced by Atiprimod in myeloma

P Neri[1,2,3], P Tassone[1,2,3], M Shammas[1], H Yasui[2], E Schipani[4], RB Batchu[1], S Blotta[1,2,3], R Prabhala[1], L Catley[2], M Hamasaki[2], T Hideshima[2], D Chauhan[2], GS Jacob[5], D Picker[5], S Venuta[3], KC Anderson[2] and NC Munshi[1,2]

[1]*Jerome Lipper Multiple Myeloma Center, Department of Adult Oncology, Dana-Farber Cancer Institute, Harvard Medical School, Boston, MA, USA;* [2]*Boston VA Healthcare System, Department of Medicine, Harvard Medical School, MA, USA;* [3]*Department of Experimental and Clinical Medicine, University of 'Magna Græcia' and Cancer Center, Catanzaro, Italy;* [4]*Endocrine Unit, Massachusetts General Hospital, Boston, MA, USA and* [5]*Callisto Pharmaceuticals Inc., New York, NY, USA*

Atiprimod (Atip) is a novel oral agent with anti-inflammatory properties. Although its *in vitro* activity and effects on signaling in multiple myeloma (MM) have been previously reported, here we investigated its molecular and *in vivo* effects in MM. Gene expression analysis of MM cells identified downregulation of genes involved in adhesion, cell-signaling, cell cycle and bone morphogenetic protein (BMP) pathways and upregulation of genes implicated in apoptosis and bone development, following Atip treatment. The pathway analysis identified integrin, TGF-β and FGF signaling as well as Wnt/β-catenin, IGF1 and cell-cycle regulation networks as being most modulated by Atip treatment. We further evaluated its *in vivo* activity in three mouse models. The subcutaneous model confirmed its *in vivo* activity and established its dose; the SCID-hu model using INA-6 cells, confirmed its ability to overcome the protective effects of BM milieu; and the SCID-hu model using primary MM cells reconfirmed its activity in a model closest to human disease. Finally, we observed reduced number of osteoclasts and modulation of genes related to BMP pathways. Taken together, these data demonstrate the *in vitro* and *in vivo* antitumor activity of Atip, delineate potential molecular targets triggered by this agent, and provide a preclinical rational for its clinical evaluation in MM.
Leukemia (2007) **21,** 2519–2526; doi:10.1038/sj.leu.2404912; published online 20 September 2007
Keywords: atiprimod; multiple myeloma; SCID-hu model; experimental treatment; gene expression profile; bone effects

Introduction

Multiple myeloma (MM) is a B-cell malignancy characterized by clonal accumulation of malignant plasma cells in bone marrow (BM). The BM microenvironment plays a critical role in promoting MM cell growth, survival, migration and development of drug resistance.[1] These findings have provided a framework for novel therapeutic strategies targeting both tumor cells and their BM microenvironment.[1,2] However, despite recent advances in the understanding of MM biology and the availability of new agents, such as thalidomide,[3] revlimid[4] and bortezomib,[5] which have improved responses and survival,[6] MM remains incurable and novel treatments are urgently needed. Atiprimod (Atip) is an Azaspirane cationic amphiphilic compound (*N-N*-diethyl-8,8-dipropyl-2-azaspiro [4.5] decane-2-propanamine), with anti-inflammatory activity in a number of experimental models of autoimmune disease and transplantation.[7,8] Atip inhibits the inflammatory response and preserves bone integrity in murine models of rheumatoid arthritis (RA),[9–12] targets macrophages, inhibits phospholipase A and C in rat alveolar macrophages[13,14] and exhibits antiproliferative and antiangiogenic activities in human cancer models.[15–17] Importantly, we have previously reported that Atip inhibits MM cell growth, induces caspase-mediated apoptosis, blocks the phosphorylation of Jak2/STAT3 and NF-kB, and downregulates the antiapoptotic proteins BCL-2, Bcl-X_l and Mcl-1[16,17] in MM cells. To further explore the anti-MM potential of Atip, we here investigate the specific signaling pathways perturbated by Atip in IL-6 dependent (INA-6) as well as independent (OPM1) MM cells, and evaluate the *in vivo* activity of this agent in three different SCID mouse models of human MM that provides a preclinical framework for its clinical evaluation in MM patients.

Correspondence: Dr NC Munshi, Jerome Lipper Multiple Myeloma Center, Department of Adult Oncology, Dana-Farber Cancer Institute, 44 Binney Street, Boston, MA 02115, USA.
E-mail: nikhil_munshi@dfci.harvard.edu
Received 29 April 2007; revised 17 July 2007; accepted 20 July 2007; published online 20 September 2007

Materials and methods

Drug

Atip was provided by Callisto Pharmaceuticals Inc. (New York, NY, USA) as powder, and was dissolved in PBS (GIBCO, Grand Island, NY, USA) at a final concentration of 10 mM and then stored in aliquots at −20° until use, to avoid multiple freeze–thaw cycles.

MM cell lines and primary patients cells

OPM1 and INA-6 human MM cell lines were kindly provided by Dr Edward Thompson (University of Texas Medical Branch, Galveston, TX, USA) and Burger[18] (University of Erlangen-Nuernberg, Erlangen, Germany), respectively. The IL-6 independent OPM1 was cultured in RPMI 1640 media (GIBCO) containing 10% fetal bovine serum, 2 mM L-glutamine (GIBCO), 100 U ml^{-1} penicillin and 100 μg ml^{-1} streptomycin (GIBCO). The IL-6 dependent INA-6 cell line was cultured in the presence of 2.5 ng ml^{-1} of human recombinant IL-6 (R&D Systems Inc., Minneapolis, MN, USA). BM aspirates were obtained from MM patients following informed consent, subjected to Ficoll–Hypaque density gradient centrifugation and mononuclear cells were separated and suspended in RPMI 1640 media (GIBCO) containing 20% fetal bovine serum, 2 mM L-glutamine (GIBCO), 100 U ml^{-1} penicillin and 100 μg ml^{-1} streptomycin (GIBCO).

Cell proliferation assay

DNA synthesis was measured by tritiated thymidine uptake [^{3}H-TdR] (NEN Life Science Products, Boston, MA, USA). Briefly, MM cells (2×10^4 cells per well) were incubated in 96-well culture plates (Costar, Cambrige, MA, USA) in the presence of

different concentrations of Atip for 24 or 48 h at 37 °C. Cells were pulsed with ^{3}H-TdR (0.5 mCi (0.185 MBq) per well), harvested onto glass filter with an automatic cell harvester (Cambridge Technology, Cambridge, MA, USA) and uptake measured using the LKB β-plate scintillation counter (Wallac, Gaithersburg, MD, USA). All experiments were performed in triplicates.

Colorimetric survival assay

Colorimetric assays were also performed to evaluate cell survival using a tetrazolium assay (CellTiter 96 Non-Radioactive Cell Proliferation Assay; Promega, Madison, WI, USA). MM cells (1×10^4 per well) were incubated in 96-well plates in 100 µl RPMI media containing 10% fetal bovine serum, L-glutamine and antibiotics and treated as indicated. At the end of each treatment, cells were incubated with 150 µl dye solution and incubated at 37 °C for 4 h. A solubilization/stop solution was then added to each well under vigorous pipetting to dissolve the formazan crystals. Absorbance readings at a wavelength of a 570 nm were obtained with a spectrophotometer (Molecular Devices, Sunnyvale, CA, USA), and cell viability was estimated as percentage of untreated controls.

Gene expression and microarray data analysis

INA-6 and OPM1 cells (2×10^6) were exposed to Atip at the IC_{50} dose for 24 h. Total RNA was isolated utilizing an 'Rneasy' kit (Qiagen Inc., Valencia, CA, USA) and gene expression profile was evaluated using the HG-U133A array chip (Affymetrix, Santa Clara, CA, USA), representing approximately 33 000 human genes. GeneChip arrays were scanned on a Gene Array Scanner (Affymetrix). Normalization of arrays and calculation of expression value were performed using the DNA-Chip Analyzer.[19] The Invariant Set Normalization method was used to normalize arrays at probe level to make them comparable, and the model-based method was used for probe selection and to compute expression values.[19] These expression levels were assigned standard errors based on replicates, which were subsequently used to compute 90% confidence intervals of fold changes in inter-group comparisons. The lower confidence bounds of 'fold change' were consecutive estimates of the actual changed. Expression of key genes involved in apoptosis, adhesion, signal transduction and cell-cycle control was analyzed. We performed assays in duplicate and repeated each experiment twice.

Western blot analyses

INA-6 and OPM1 cells were exposed to Atip at the IC_{50} dose for 12 or 24 h, harvested, washed and lysed using lysis buffer: 50 mM Tris-HCl (pH 7.4), 150 mM NaCl, 1% NP-40, 10 mM sodium pyrophosphate, 5 mM EDTA, 1 mM ethylene glycol tetraacetic acid (EGTA), 2 mM Na_3VO_4, 5 mM NaF, 1 mM PMSF, 5 µg ml^{-1} leupeptin and 5 µg ml^{-1} aprotinin. Whole cell lysates (10–20 µg per lane) were subjected to SDS–PAGE separation, transferred to polyvinylidene difluriode (PVDF) membranes (Bio-Rad Laboratories, Hercules, CA, USA) and immunoblotted with anti-p-21 antibody (Cell Signaling, Beverly, MA, USA).

Pathway analysis

In order to analyze all cellular pathways modulated by Atip, we examined a number of genes with altered expression in known pathway networks using a network-mapping tool, the Ingenuity Systems Software (Ingenuity Systems, Mountain View, CA, USA), which is able to explore the most relevant networks of gene interactions from experimental data. A cutoff of 2 was set to identify genes with significant regulation (Focus Genes, Ingenuity Pathways analysis, 2003 release, Ingenuity Systems). The use of this stringent statistical threshold of 2, comparing treated versus control MM cells resulted in the identification of 1357 genes for INA-6 and 1372 for OPM1. The identified genes were mapped to all networks available in the Ingenuity database and were then ranked by score. The score is the probability that a collection of genes equal to or greater than the number in a network could be achieved by chance alone. Genes with maximum score are the most significantly modulated. Pathways with the higher score of 38 for INA-6 and 37 for OPM1 have been used to form a composite network, representing the underlying biology of the process.

In vivo *activity: animals*

CB-17 SCID-mice were obtained from Taconic (Germantown, NY, USA), maintained and monitored in our animal research facility. All animal studies were conducted according to protocols approved by the Institutional Animal Care and Use Committee. Animals were killed when their tumors reached 2 cm in diameter or when paralysis or major compromise in their quality of life occurred.

Human MM xenograft murine model

CB 17 SCID-mice were subcutaneously (s.c.) inoculated in the interscapular area with 2.5×10^6 OPM1 cells in 100 µl of RPMI-1640 medium. When the tumor was measurable, approximately 3 weeks after the MM cells injection, mice were treated with Atip intraperitoneally (i.p.) at 20, 30 and 50 mg kg^{-1} on alternate days for 7 days. Tumor size was measured every 3 days in two dimensions using an electronic caliper, and the tumor volume was calculated using the following formula: $V = 0.5a \times b^2$, where a and b are the long and short diameter of the tumor, respectively.

SCID-hu models of human MM

Human fetal long bone grafts were s.c. implanted into SCID mice (SCID-hu), as previously described.[20,21] In the SCID-hu INA-6 model, 4 weeks following bone implantation, 2.5×10^6 INA-6 MM cells were injected directly into the human BM cavity in the SCID-hu mice in a final volume of 100 µl of RPMI-1640 medium. An increase in the levels of soluble human IL-6 receptor (shuIL-6R), released by INA-6 cells, was used as an indicator of MM cell growth and burden of disease in SCID-hu mice. Mouse sera were serially measured for shuIL-6R levels by an enzyme-linked immunosorbent assay (ELISA, R&D Systems Inc.). Mice developed measurable serum shuIL-6R approximately 4 weeks following INA-6 cell injection, and were then treated i.p. with vehicle alone or Atip at 40 mg kg^{-1} every other day for 3 weeks. Following treatments, blood samples were collected and analyzed.

In the SCID-hu mice injected with primary patient MM cells, mice were produced as previously described,[20,21] and received 5×10^6 BM cells from a MM patient, directly into the human bone chip in a final volume of 100 µl of RPMI-1640 medium, approximately 4 weeks following the bone implant. Increasing levels of circulating human paraprotein in mice sera were monitored and used as an indicator of tumor engraftment and MM growth. Levels of human immunoglobulin G (IgG), κ and λ light chains were determined by ELISA (Bethyl, Montgomery,

TX, USA). When MM engraftment was detectable (IgG κ or λ positive), mice were treated with i.p. Atip (50 mg kg^{-1}) or vehicle alone (PBS) on alternate days for 4 weeks.

Histological analysis

Analysis was performed on decalcified fetal bone chips retrieved from SCID-hu mice, following 3 months of weekly i.p. treatment with Atip at 40 mg kg^{-1}. Tissues were fixed in 3.7% formaldehyde/PBS overnight at 4 °C, processed, embedded in paraffin and sections were obtained. *In situ* hybridizations were performed using complementary 35S-labeled riboprobes as described previously.[22]

Statistical analysis

Statistical significances of differences were determined by using Student's *t*-test. The minimal level of significance was $P<0.05$.

Results

Perturbation of growth and survival genes by Atip

We have previously reported that Atip induces *in vitro* cytotoxicity via poly (ADP-ribose) polymerase (PARP) cleavage and caspase-mediated apoptosis in conventional drug-sensitive (MM.1S, RPMI8226, U266, INA-6) and resistant (MM.1R, RPMI-LR5) MM cell lines as well as primary tumor cells with an IC_{50} in the range of 0.5–1.25 μM.[16] As IL-6 dependent (INA-6) and independent (OPM1) MM cells are used in our animal models, we first confirmed, using ^{3}H-TdR uptake as well as MTT assays, that Atip inhibits growth and survival of INA-6 as well as OPM1 cell lines *in vitro* in a time and dose-dependent manner, with an IC_{50} in the range of 0.5–0.75 μM (Figures 1a and b). To characterize the molecular sequelae triggered by Atip in MM cells, we evaluated changes in global gene expression profile in MM cells following 24 h exposure to the drug. Both INA-6 and OPM1 cells were treated with Atip at the IC_{50} dose for 24 h, RNA isolated and the gene expression profile analyzed using HG-U133A GeneChip arrays (Affymetrix), which represents approximately 33 000 human genes. We focused on expression pattern of genes modulated in Atip-treated versus control MM cells. As shown in Figure 2, demonstrating data as fold change, in both INA-6 and OPM1 cells, significant upregulation was observed in genes involved in apoptosis (p21, TNF15, TRAILR3, SEMA6A, ADRA1A and v-Fos), whereas downregulation occurred in genes involved in cell cycle (TGF-β receptor II, PTPRN2 and PTPN21), adhesion (integrin β1 and 8, cadherin 3, cadherin F9 and cadherin F8) and cell signaling (MAPK5 and Nuclear receptor 2C1) pathways. Interestingly, genes involved in bone development, such as DLX5, GDF8, MMP1, LECT2, were upregulated and genes implicated in negative regulation of bone morphogenic protein signaling pathways, such as SMAD-specific E3 ubiquitin protein ligase 1 and FGFR3 were down-regulated. Since our gene array data showed that p21 is the most modulated gene in both cell lines (more than 6-fold change), we performed an immunoblot analysis to evaluate its protein levels in MM cells. As shown in Figure 3, Atip at the IC_{50} dose upregulates p21 at 12 and 24 h in both INA-6 and OPM1 cells, confirming the gene expression changes as well as its role in the apoptotic process induced by Atip.

Pathway analysis of representative genes affected by Atip

In order to analyze biological pathways affected by Atip, all genes were subjected to Ingenuity Pathway Analysis. As seen in

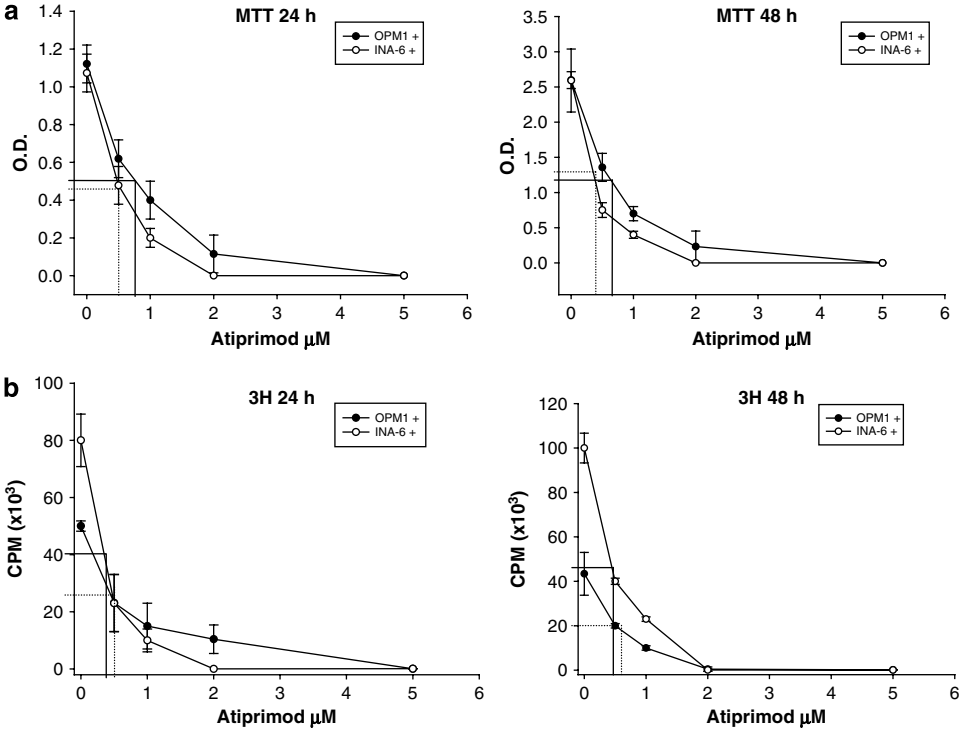

Figure 1 *In vitro* antiproliferative effect of Atiprimod (Atip) on MM cell lines. (**a**) OPM1 and INA-6 cells were cultured in control media or in the presence of Atip (0–5 μM) for indicated times. Time- and dose-dependent inhibition of proliferation was assessed by ^{3}H-TdR at 24 or 48 h. (**b**) Effect of Atip on cell survival of IL-6 dependent (INA-6) as well as independent (OPM1) MM cells was performed by MTT at 24 or 48 h. Data represent mean (±s.d.) of triplicate cultures.

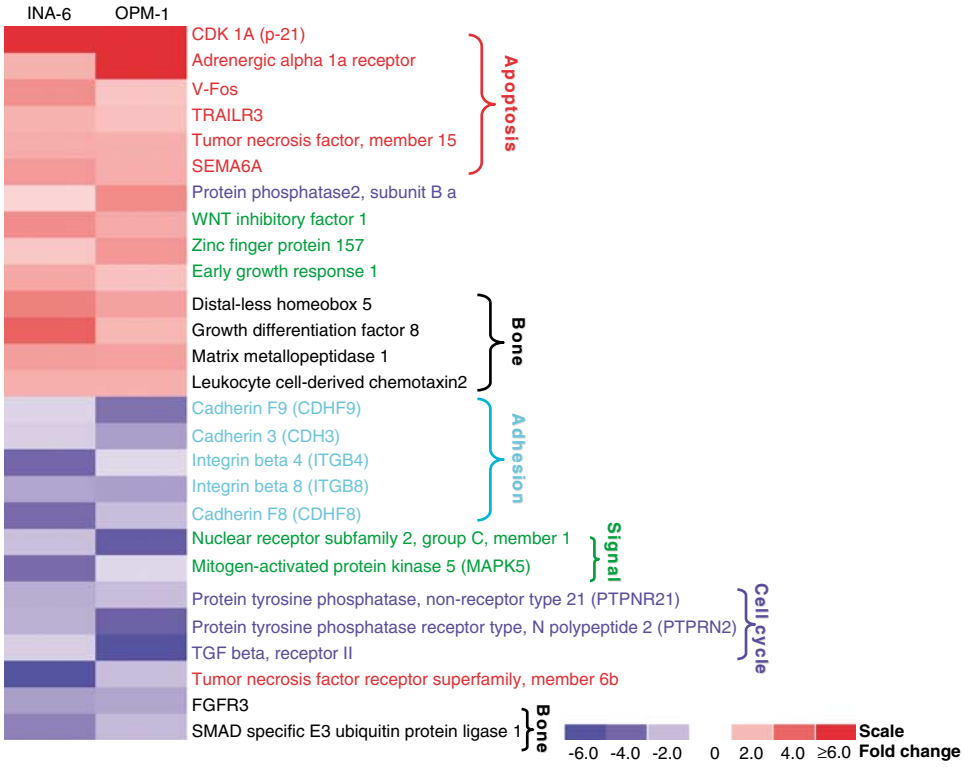

Figure 2 Gene expression profile of INA-6 and OPM1 cells after 24 h of Atip treatment. Gene expression profile of INA-6 and OPM1 MM cells treated with Atip at the IC_{50} dose for 24 h was analyzed using the HG-U133A array chip. Genes significantly induced, relative to untreated control cells (>2-fold change), in both cell lines are implicated in apoptosis, bone development as well as in cell–cell adhesion, signal transduction and cell cycle, and are shown here. We performed assays in duplicate and repeated each experiment twice.

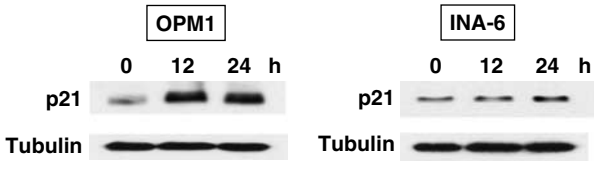

Figure 3 Atiprimod (Atip) induces upregulation of p-21 levels in MM cells. OPM1 and INA-6 cells were cultured with control media or Atip at the IC_{50} dose for 12 or 24 h. Total cell lysates were subjected to immunoblotting using anti-p21 Ab.

Figure 4, in both cell-lines G-protein, Integrin, wnt/β-catenin signaling pathways as well as IL-6, ERK/MAPK, TGF-β, FGF, IGF-1 and cell-cycle regulation pathways were most modulated following Atip treatment. In particular, the bar graph shows the number of genes modulated for each pathways by Atip in both cell lines as compared to untreated cells, based on significance obtained by the Ingenuity analysis. The highest scoring networks were selected for further analysis based on significance (*P*-value) and combined to form a composite network representing the overall molecular effect of Atip in each cell line. As shown in Figure 5, representing the principle nodes modulated by Atip in both cell lines, the genes that were most modulated were those commonly involved in cell-cycle arrest and apoptosis (TADA3L, p21, AP2A2, MAF, JUN, ERG, PPARG), integrin signaling (ITGB5, IGFBP5, ITGB8 and FN1), signal transduction (IL1R1, MAP3K13, ADRA1D, ABCC3, PDGFRB), FGF regulation (FGF2, FGFR1) and TGF-β signaling and development (GDF8, GDF15, TGF-β1, TGF-β2, SPARC, Bone morphogenic protein 2), (Figure 5). Taken together these data identify critical pathways that can explain the drug's growth inhibitory activity.

In vivo *activity of Atip in a subcutaneous and SCID-hu models of MM*

Following the identification of the major molecular pathways perturbated by Atip in MM, we next evaluated the *in vivo* activity of Atip in a subcutaneous murine model of human MM. A cohort of 21 SCID-hu were engrafted with OPM1 cells and treated with vehicle alone or Atip 20 mg kg^{-1} ($n=3$), 30 mg kg^{-1} ($n=5$) or 50 mg kg^{-1} ($n=5$) every other day i.p. (PBS, $n=8$) for 7 days. As shown in Figure 6a, mice treated with Atip at 20, 30 or 50 mg kg^{-1} showed 31, 48 and 55% growth inhibition, respectively, compared with control group, demonstrating that Atip has considerable *in vivo* activity against human MM.

In order to study the activity of Atip on MM cells growing in the context of a human BM microenvironment, we next used a SCID-hu model in which IL-6 dependent INA-6 cells are directly injected into previously implanted human fetal bone chip in SCID-mice.[23,24] A cohort of 10 SCID-hu mice bearing human bones engrafted with INA-6 cells were treated i.p. on alternate day with Atip (40 mg kg^{-1}, $n=5$) or vehicle alone (PBS, $n=5$), respectively, for 3 weeks. In this model, the anti-MM activity is analyzed by measuring the serum shuIL-6R levels, secreted by INA-6 cells. As shown in Figure 6b, Atip treatment induced significant tumor regression as compared with control mice (78% reduction in shuIL-6R, $P=0.03$). To evaluate the *in vivo* efficacy of Atip against primary patient derived MM cells, we treated SCID-hu mice previously engrafted with explanted

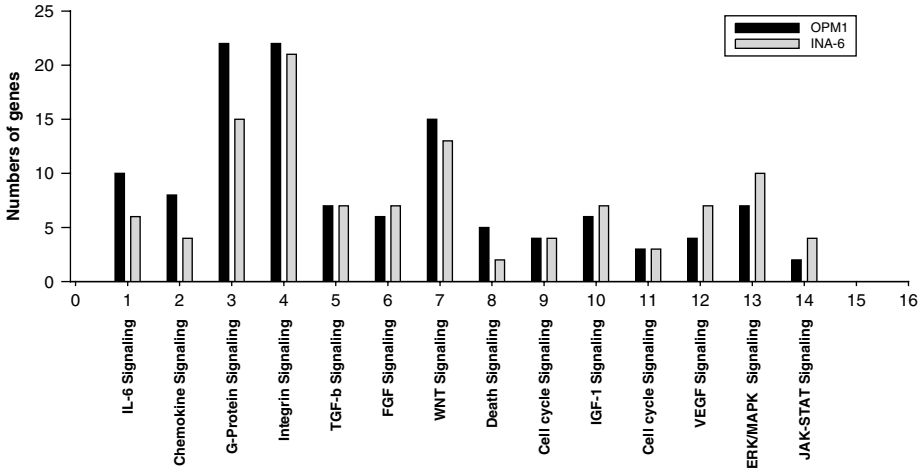

Figure 4 Functional categories of pathways modulated by Atip. To analyze biological pathways affected by Atip, all genes were subjected to Ingenuity Pathway Analysis. The bar graph shows the number of genes modulated for each pathways by Atip in OPM1 (black) and INA-6 (gray) cell lines as compared to untreated cells, based on significance and obtained by the Ingenuity analysis.

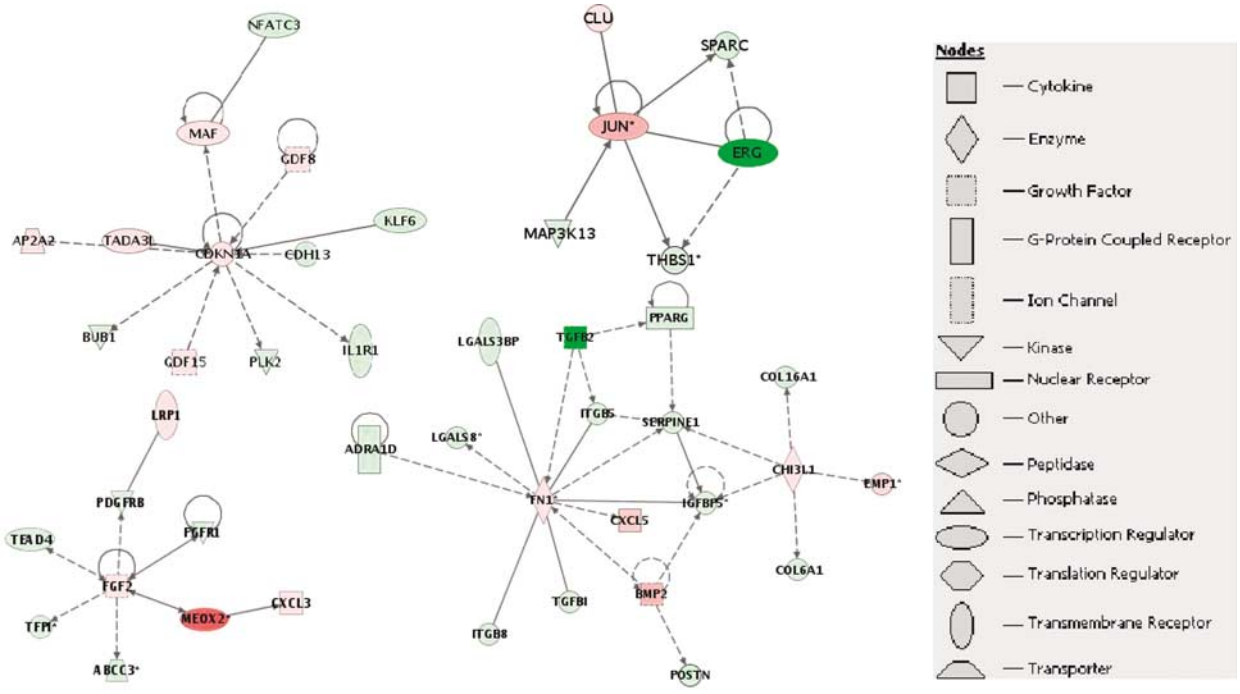

Figure 5 Pathway analysis of representative genes affected by Atip. Pathways with the higher score of 38 and 37 have been used to form a composite network representing the underlying biology of the effect. Figure shows the principle nodes in the networks affected by Atip in both cell lines. Upregulated and downregulated genes are indicated in red and green, respectively; the white color indicates genes that are not user specified, but incorporated into the networks through relationship with other genes. Continuous and discontinuous lines represent direct and indirect functional and physical interaction between genes demonstrated in literature.

primary MM cells with Atip i.p. 50 mg kg^{-1} or vehicle alone (PBS) on alternate days for 4 weeks, following the detection of human IgG κ or λ chains in mice sera. As seen in Figure 6c treatment with Atip induced a reduction in human paraprotein levels in murine sera, whereas IgG and the λ light chain continued to rise in mice treated with vehicle alone. We have treated three groups, two mice (one control and one treated) in each group injected with primary MM cells from the same patient; Figure 6c is a representative *in vivo* experiment. Taken together, these data demonstrate *in vivo* anti-MM activity of Atip against primary MM cells engrafted in the context of human BM microenvironment.

Effect of Atip on MM induced bone resorption

Previous studies have shown the ability of Atip to inhibit bone resorption in an *in vitro* assay (Badger *et al*., 1996, private communication) and protect bones from the destructive effects of the arthritis.[11] Based on these preliminary studies and our gene array data, we evaluated the *in vivo* effects of this drug on bone formation and resorption. Four SCID-hu mice, previously implanted with the bone chip, received weekly i.p. injections of Atip 40 mg kg^{-1} for 3 months. Mice were killed, bone implant retrieved and analyzed by *in situ* hybridization. As shown in Figure 6d, Atip treatment significantly decreases the osteoclasts

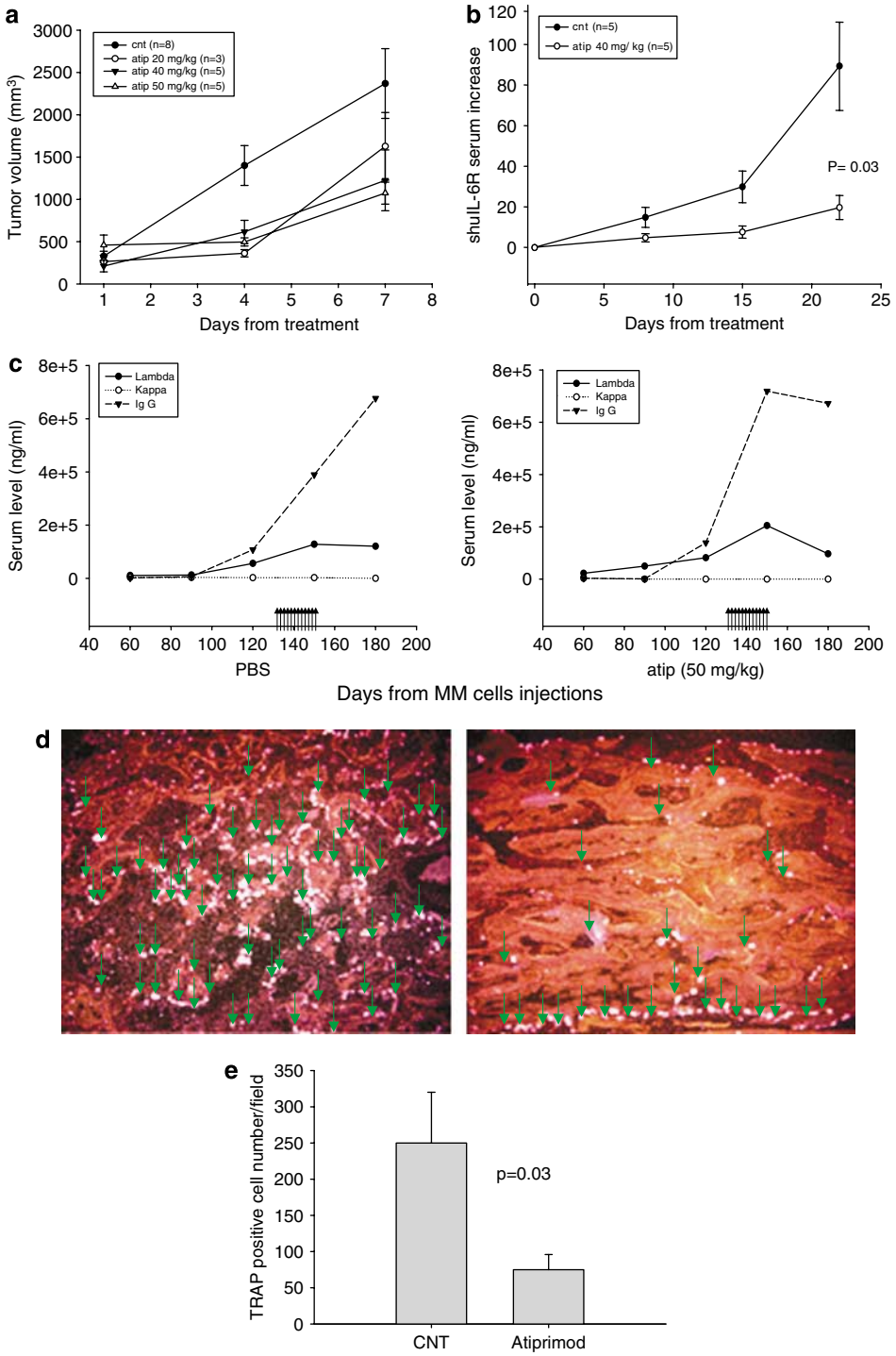

Figure 6 *In vivo* activity of Atiprimod (Atip) on MM xenograft and SCID-hu models. (**a**) CB-17 SCID mice were injected s.c. with 2×10^6 OPM1 cells. Following detection of measurable tumor, animals were treated with 20 mg kg^{-1} ($n=3$), 30 mg kg^{-1} ($n=5$) and 50 mg kg^{-1} ($n=5$) Atip i.p or vehicle alone (PBS $n=8$) on alternate days for 7 days. Tumor volume was assessed in two dimensions using an electronic caliper and the volume was expressed in mm^3 using the following formula $V=0.5a \times b^2$ where a and b are the long and short diameter of the tumor, respectively. Tumor volume was evaluated every 3 days until the day of killing or death. (**b**) SCID-hu mice engrafted with INA-6 cells in human bone chip were monitored for tumor growth by serial serum measurements of shuIL-6R as a measure of MM cell growth. Mice were treated with Atip i.p. at 40 mg kg^{-1}, ($n=5$) or vehicle alone ($n=5$) on alternate days for 3 weeks and the shuIL-6R levels were determined every week. (**c**) SCID-hu mice were bled at the indicated time points after inoculation of primary MM cells, and monitored for changes in levels of human serum paraprotein (IgG, κ or λ chains) as an indicator of disease burden. The animals were treated with Atip (50 mg kg^{-1}, $n=2$) i.p. or with vehicle alone (PBS, $n=2$) on alternate days for 4 weeks when the level of human serum paraproteins became detectable. We have treated three animals in each group, every two mice (one control and one treated) were injected with primary MM cells from one of three different patients and the Figure is a representative *in vivo* experiment. Arrows indicate the days of treatment. (**d**) Effect of Atip on MM induced bone resorption. To evaluate *in vivo* effects of Atip on bone formation and resorption, four SCID-hu mice were killed after 3 months of weekly i.p. treatment with Atip (40 mg kg^{-1}). The decalcified bone chips were probed with 35S-labeled antisense riboprobe, detecting TRAP mRNA in serial sections. The bright spots identifies TRAP + osteoclasts. (**e**) Note the dramatic decrease of TRAP positive osteoclasts, in Atip-treated specimens versus controls. Table 1 shows, as fold change, genes related to the BMP pathways, modulated following Atip treatment in both cell lines.

number in Atip-treated mice compared to the control group, suggesting effect of Atip on bone remodeling. In particular, the number of multinucleated TRAP-positive cells was 250 in human rudiments from control mice, bearing MM cells but treated with vehicle alone and 75 per field ($P=0.03$) in mice treated with Atiprimod when compared to the control (Figure 6e).

Finally, the Table 1 shows, as fold change, genes related to the bone morphogenic protein pathways, modulated following Atiprimod treatment in both cell lines when compared to the control. In particular, significant upregulation was observed in several genes, members of the bone morphogenetic protein (BMP) family, involved in bone development, such as BMP-1, BMPR1A, BMP-2, BMP-5, GDF15, GDF8, GDF5 and as well as in genes implicated in the prevention of bone resorption, such as calcitonin (CALCA) and osteoprotegerin (OPG).

Discussion and conclusion

In the past few years, considerable progress has been made in the development of new drugs for MM treatment by the identification of key molecular mechanisms that play a critical role in the growth and survival of this cancer. A complex network of cytokines, chemokines and cell surface molecules modulate the interaction between MM cells and the BM microenvironment thereby regulating MM cell proliferation, growth, survival and development of drug resistance.[25–27] This has led to development of novel agents that target not only MM cells, but also the BM *milieu*, and are able to overcome resistance to conventional therapies.[28]

In this report, we investigated *in vitro* molecular mechanisms and *in vivo* activity of Atip, as a therapeutic agent in MM. Previous studies performed in our laboratory as well as by others have demonstrated *in vitro* activity of Atip on MM cell lines and its ability to block Jak2/STAT3 and NF-kB, signaling pathways which play an important role for MM growth and survival,[16,17] but its effect on expression profile has not been previously explored. Based on these data, in this study, we selected 24 h a time point that captures maximal effect of the drug and used IL-6 dependent (INA-6) and independent (OPM1) MM cells in order to focus on changes in gene expression profiles induced by Atip. We identified a specific pattern of transcriptional events induced by Atip in MM cells that leads to eventual growth arrest and apoptosis. Atip was found to induce pro-apoptotic genes (TNF15, TRAILR3, p21 and v-Fos) and to downregulate transcripts essential for the cell-cycle progression (PTPNR21, PTPRN2, TGF-β2), adhesion and signal transduction (ITGB4 and 8, CDH3 and CDHF9, MAPK5 and nuclear receptor 2C1). The upregulation of transcripts implicated in apoptosis, such as the death ligands TNF15, and TRAILR3, are consistent with previous studies showing the pro-apoptotic role of these molecules.[29,30] Moreover, the upregulation of p-21, a known mediator of cell-cycle arrest and apoptosis,[31] shown by both gene array data and western blot analysis, could partially explain the activity of Atip on MM cells. Using the Ingenuity Pathway Analysis on cells treated with Atip, we identified genes and pathways that are of specific interest in MM biology. Specifically, the pathway mapping analysis identified the modulation of genes involved in integrin signaling (ITGB5, IGFBP5, ITGB8 and FN1), important in mediating MM cell adhesion to the stroma[32] and in the development of drug resistance.[33] Similarly, we observed modulation of FGF and TGF-β signaling (FGF2, FGFR1 and TGF-β2, GDF8, GDF15, TGF-β1, TGF-β2, SPARC and BMP2) involved in promoting MM cell growth and survival[34] which may contribute to the overall effect of Atip on MM cells. Taken together our data show the ability of Atip to perturb critical pathways that may explain the drug's growth inhibitory activity in MM and establish a framework to design combination therapies with conventional and/or novel antitumor agents. Importantly, we confirmed the *in vivo* activity of Atip using three different murine models of human MM, including a conventional subcutaneous model of human MM and two different SCID-hu models that engraft human MM cells in the context of their specific human BM *milieu*. Whereas the subcutaneous xenograft model confirmed *in vivo* activity of Atip in MM and established its dose and activity, the SCID-hu INA-6 model,[23] confirmed the drug's ability to overcome the protective effects of the BM *milieu* on MM cell growth, survival and drug resistance.[2] The drug's activity in the SCID-hu model using the primary patient MM cells, a model that accurately recapitulates the human disease, reconfirmed the activity of Atip against human MM engrafted in the context of human BM microenvironment. Therefore, our *in vivo* data demonstrated the ability of Atip to induce a dose-dependent antitumor effect in all three murine models. Bone disease is a significant clinical component of MM presentation.[35] Lytic bone lesions and their associated complications are the major causes of morbility in MM. The predominant feature of this complication is an increased osteoclast number and activity, leading to increased bone resorption along with decreased osteoblast activity.[36] Of particular interest was the observed reduction in the number of osteoclasts following Atip treatment and the upregulation of several genes related to the BMP pathways in MM-treated cells versus control. In particular Atip was found to induce several members of the BMP family , critical factors to promote cartilage and bone formation.[37] Similarly, we observed upregulation of the soluble decoy receptor OPG and CALCA involved in the negative regulation of bone resorption,[38] suggesting a potential role of this agent in MM bone disease. Based on these data, a detailed evaluation of Atip's effects on osteoclast number and function at molecular and signaling level is warranted to define its use in bone disease. In conclusion, the present report demonstrates the *in vitro* anti-MM activity of Atip; it delineates biological targets, defines molecular pathways triggered by this drug and confirms strong *in vivo* evidence of its activity in preclinical models of MM. Taken together our data provide a rationale for its clinical evaluation in MM.

Table 1 Effect of Atip on genes related to the BMP pathways

Gene	*Locus link*	*Fold change*	*Cell line*
CALCA	796	12.4	INA-6
BMPR1A	657	8.7	INA-6
GDF15	9518	3.8	INA-6
GDF8	2660	3.8	INA-6
BMP-1	649	2.6	INA-6
BMP-2	650	13.6	OPM1
OPG	4982	4	OPM1
BMP-5	653	2	OPM1
GDF5	8200	2	OPM1

Abbreviations: Atip, atiprimod; BMP, bone morphogenetic protein; CALCA, calcitonin; GDF, growth and differentiation factor; OPG, osteoprotegerin.

Acknowledgements

We gratefully acknowledge Professor Pierosandro Tagliaferri (Magna Graecia University, Catanzaro, Italy) for helpful

discussions and critically reviewing this paper. This work is supported by Multiple Myeloma Research Foundation Awards (MAS, NCM and KCA); Department of Veterans Affairs merit review grant and the Leukemia and Lymphoma Society Scholar in Translational Research Award (NCM); NIH Grants P50-100707 and PO1-78378 (KCA, NCM); as well as NIH Grant RO1-50947 and the Doris Duke Distinguished Clinical Research Scientist Award (KCA).

References

1 Hideshima T, Chauhan D, Podar K, Schlossman RL, Richardson P, Anderson KC. Novel therapies targeting the myeloma cell and its bone marrow microenvironment. *Semin Oncol* 2001; **28**: 607–612.
2 Hideshima T, Anderson KC. Molecular mechanisms of novel therapeutic approaches for multiple myeloma. *Nat Rev Cancer* 2002; **2**: 927–937.
3 Barlogie B, Tricot G, Anaissie E. Thalidomide in the management of multiple myeloma. *Semin Oncol* 2001; **28**: 577–582.
4 Barlogie B. Thalidomide and CC-5013 in multiple myeloma: the University of Arkansas experience. *Semin Hematol* 2003; **40** (Suppl 4): 33–38.
5 Richardson PG, Sonneveld P, Schuster MW, Irwin D, Stadtmauer EA, Facon T *et al.* Bortezomib or high-dose dexamethasone for relapsed multiple myeloma. *N Engl J Med* 2005; **352**: 2487–2498.
6 Jemal A, Tiwari RC, Murray T, Ghafoor A, Samuels A, Ward E *et al.* Cancer statistics, 2004. *CA Cancer J Clin* 2004; **54**: 8–29.
7 Albrightson-Winslow CR, Brickson B, King A, Olivera D, Short B, Saunders C *et al.* Beneficial effects of long-term treatment with SK&F 105685 in murine lupus nephritis. *J Pharmacol Exp Ther* 1990; **255**: 382–387.
8 Hancock WW, Schmidbauer G, Badger AM, Kupiec-Weglinski JW. SK&F 105685 suppresses allogeneicallly induced mononuclear and endothelial cell activation and cytokine production and prolongs rat cardiac allograft survival. *Transplant Proc* 1992; **24**: 231–232.
9 Fan PY, Albrightson CR, Howell DN, Best C, Badger AM, Coffman TM. The azaspirane SKF 105685 ameliorates renal allograft rejection in rats. *J Am Soc Nephrol* 1993; **3**: 1680–1685.
10 Badger AM, Swift BA, Webb EF, Clark RK, Bugelski PJ, Griswold DE. Beneficial effects of SK&F 105685 in rat adjuvant arthritis: prophylactic and therapeutic effects on disease parameter progression. *Int J Immunopharmacol* 1993; **15**: 343–352.
11 High WB, Bugelski PJ, Nichols ME, Swift BA, Solleveld HA, Badger AM. Effects of a novel azaspirane (SK&F 105685) on arthritic lesions in the adjuvant Lewis rat: attenuation of the inflammatory process and preservation of skeletal integrity. *J Rheumatol* 1994; **21**: 476–483.
12 Bradbeer JN, Kapadia RD, Sarkar SK, Zhao H, Stroup GB, Swift BA *et al.* Disease-modifying activity of SK&F 106615 in rat adjuvant-induced arthritis. Multiparameter analysis of disease magnetic resonance imaging and bone mineral density measurements. *Arthritis Rheum* 1996; **39**: 504–514.
13 Badger AM, Newman-Tarr TM, Satterfield JL. Selective immunomodulatory activity of SK&F 106615, a macrophage-targeting antiarthritic compound, on antibody and cellular responses in rats and mice. *Immunopharmacology* 1997; **37**: 53–61.
14 Handler JA, Badger A, Genell CA, Klinkner AM, Kassis S, Waites CR *et al.* Selective inhibition of phospholipases by atiprimod, a macrophage targeting antiarthritic compound. *Toxicol Appl Pharmacol* 1999; **159**: 9–17.
15 Shailubhai K, Dheer S, Picker D, Kaur G, Sausville EA, Jacob GS. Atiprimod is an inhibitor of cancer cell proliferation and angiogenesis. *J Exp Ther Oncol* 2004; **4**: 267–279.
16 Hamasaki M, Hideshima T, Tassone P, Neri P, Ishitsuka K, Yasui H *et al.* Azaspirane (*N*-*N*-diethyl-8,8-dipropyl-2-azaspiro [4.5] decane-2-propanamine) inhibits human multiple myeloma cell growth in the bone marrow milieu *in vitro* and *in vivo*. *Blood* 2005; **105**: 4470–4476.
17 Amit-Vazina M, Shishodia S, Harris D, Van Q, Wang M, Weber D *et al.* Atiprimod blocks STAT3 phosphorylation and induces apoptosis in multiple myeloma cells. *Br J Cancer* 2005; **93**: 70–80.
18 Burger R, Guenther A, Bakker F, Schmalzing M, Bernand S, Baum W *et al.* Gp130 and ras mediated signaling in human plasma cell line INA-6: a cytokine-regulated tumor model for plasmacytoma. *Hematol J* 2001; **2**: 42–53.
19 Li C, Wong WH. Model-based analysis of oligonucleotide arrays: expression index computation and outlier detection. *Proc Natl Acad Sci USA* 2001; **98**: 31–36.
20 McCune JM, Namikawa R, Kaneshima H, Shultz LD, Lieberman M, Weissman IL. The SCID-hu mouse: murine model for the analysis of human hematolymphoid differentiation and function. *Science* 1988; **241**: 1632–1639.
21 Urashima M, Chen BP, Chen S, Pinkus GS, Bronson RT, Dedera DA *et al.* The development of a model for the homing of multiple myeloma cells to human bone marrow. *Blood* 1997; **90**: 754–765.
22 Schipani E, Lanske B, Hunzelman J, Luz A, Kovacs CS, Lee K *et al.* Targeted expression of constitutively active receptors for parathyroid hormone and parathyroid hormone-related peptide delays endochondral bone formation and rescues mice that lack parathyroid hormone-related peptide. *Proc Natl Acad Sci USA* 1997; **94**: 13689–13694.
23 Tassone P, Neri P, Carrasco DR, Burger R, Goldmacher VS, Fram R *et al.* A clinically relevant SCID-hu *in vivo* model of human multiple myeloma. *Blood* 2005; **106**: 713–716.
24 Tassone P, Neri P, Burger R, Savino R, Shammas M, Catley L *et al.* Combination therapy with interleukin-6 receptor superantagonist Sant7 and dexamethasone induces antitumor effects in a novel SCID-hu *in vivo* model of human multiple myeloma. *Clin Cancer Res* 2005; **11**: 4251–4258.
25 Clark SC, Kamen R. The human hematopoietic colony-stimulating factors. *Science* 1987; **236**: 1229–1237.
26 Sieff CA. Biology and clinical aspects of the hematopoietic growth factors. *Annu Rev Med* 1990; **41**: 483–496.
27 Anderson K. Advances in the biology of multiple myeloma: therapeutic applications. *Semin Oncol* 1999; **26** (Suppl 13): S10–S22.
28 Hideshima T, Richardson P, Anderson KC. Novel therapeutic approaches for multiple myeloma. *Immunol Rev* 2003; **194**: 164–176.
29 Gupta S. Molecular steps of tumor necrosis factor receptor-mediated apoptosis. *Curr Mol Med* 2001; **1**: 317–324.
30 Bharti AC, Aggarwal BB. Ranking the role of RANK ligand in apoptosis. *Apoptosis* 2004; **9**: 677–690.
31 Sherr CJ, Roberts JM. CDK inhibitors: positive and negative regulators of G1-phase progression. *Genes Dev* 1999; **13**: 1501–1512.
32 Sanz-Rodriguez F, Teixido J. VLA-4-dependent myeloma cell adhesion. *Leuk Lymphoma* 2001; **41**: 239–245.
33 Damiano JS, Dalton WS. Integrin-mediated drug resistance in multiple myeloma. *Leuk Lymphoma* 2000; **38**: 71–81.
34 Hideshima T, Podar K, Chauhan D, Anderson KC. Cytokines and signal transduction. *Best Pract Res Clin Haematol* 2005; **18**: 509–524.
35 Callander NS, Roodman GD. Myeloma bone disease. *Semin Hematol* 2001; **38**: 276–285.
36 Roodman GD. Pathogenesis of myeloma bone disease. *Blood Cells Mol Dis* 2004; **32**: 290–292.
37 Wozney JM. Bone morphogenetic proteins. *Prog Growth Factor Res* 1989; **1**: 267–280.
38 Sezer O, Heider U, Zavrski I, Kuhne CA, Hofbauer LC. RANK ligand and osteoprotegerin in myeloma bone disease. *Blood* 2003; **101**: 2094–2098.